JTE HCM-UTE
ISSN: 2615-9740

JOURNAL OF TECHNICAL EDUCATION SCIENCE
Ho Chi Minh City University of Technology and Engineering
Website: https://jte.edu.vn
Email: jte@hcmute.edu.vn

Compact Symmetric Quad-Arm Meander-Line RFID Tag Antenna for Metallic Surface Applications

Minh Tan Nguyen*
Ho Chi Minh City University of Technology (HCMUT), VNU-HCMC, Vietnam

*Corresponding author. *Email: nmtan@hcmut.edu.vn*

ARTICLE INFO

Received: 01/10/2025
Revised: 11/11/2025
Accepted: 19/11/2025
Published online: 03/03/2026

KEYWORDS

Metal tag antenna;
RFID chip;
Impedance matching;
RFID tag antenna;
Meander-line patch.

ABSTRACT

A miniaturized UHF RFID tag antenna designed for use with the Ucode 8/8m IC chip—characterized by an input impedance of 15 – j217 Ω at 915 MHz—is introduced. To ensure optimal power transfer, the antenna geometry was meticulously refined to achieve conjugate impedance matching with the chip. The final total structure, measuring 50 × 50 × 0.4 mm³, delivers a power transmission coefficient of up to 95% and supports a read range exceeding 8.0 meters when operating under an effective isotropic radiated power (EIRP) of 4.0 W. Performance testing was carried out with the tag affixed to a 250 × 250 mm² metal surface, demonstrating reliable functionality in metallic environments. The antenna is tuned to operate within the FCC-designated UHF RFID frequency band (902–928 MHz), suitable for deployment in North America and Vietnam. Experimental measurements closely matched full-wave simulation results, validating both the impedance-matching strategy and the overall design efficiency.

Doi: https://doi.org/10.54644/jte.2026.2012

1. Introduction

Radio frequency identification (RFID) technology has been widely adopted in numerous applications, including toll collection systems, logistics and distribution management, the Internet of Things (IoT), supply chain tracking, and security monitoring [1], [2]. A typical passive RFID tag consists of an antenna and an integrated circuit (IC) chip, usually operating in the ultrahigh frequency (UHF) band. Within this band, tags can achieve longer reading distances at relatively low cost, which makes UHF systems attractive for large-scale deployments [3], [4].

Despite these advantages, the performance of tag antennas deteriorates significantly when they are attached directly to metallic objects. The conductive surface alters the electromagnetic field distribution, leading to degraded input impedance, reduced power transmission coefficient (PTC), lower gain, and distorted radiation characteristics. To address these challenges, various antenna designs have been proposed. One approach employs artificial magnetic conductors (AMCs) to enhance antenna gain and radiation properties. In such designs, the radiating patch is positioned above an AMC ground plane [5]–[8]. While effective, AMC-based antennas typically involve complicated layouts, increased physical dimensions, and higher fabrication costs, which limit their practicality for compact, low-cost RFID applications.

To achieve a thinner profile, planar inverted-F antennas (PIFAs) have been introduced. PIFA designs rely on high-impedance surfaces to suppress metallic effects [9], [10]. However, conjugate impedance matching between the antenna and the IC chip remains a challenge because most RFID chips are designed with high quality factors for improved sensitivity, leading to narrow bandwidths and complex impedance characteristics [11]–[13]. Several methods, such as loading bars and conductive sheets, have been investigated to improve impedance matching [14], [15], but they often suffer from low radiation efficiency. Via-loaded patches have also been proposed to enhance efficiency [16], [17], though their performance depends strongly on the feed-point configuration and the placement of shorting vias, making tuning and fabrication more difficult and costly.

Another strategy involves folded patch antennas derived from the PIFA concept. For instance, a compact folded-patch tag antenna designed for metallic mounting was reported in [18]. This structure, formed by splitting a square patch into two rectangular sections and connecting them to ground through multiple thin inductive stubs, reduces antenna size but introduces practical limitations. Specifically, the use of aluminum patches with adhesive bonding degrades reading performance due to surface oxidation [19]. In addition, folded structures often require extra ground planes or stacked radiating layers, which increase design complexity and antenna volume [20], [21]. Although more robust folded configurations without additional patch layers have been demonstrated [22], challenges remain, such as the reliance on shorting stubs that complicate resonance tuning.

In summary, although many existing RFID tag antennas for metallic surfaces have been reported – such as AMC-based structures, folded or via-loaded patches, and loop-type or inverted-F configurations – they typically suffer from one or more limitations including large thickness, complex multi-layer construction, or difficult impedance tuning. In contrast, the proposed design introduces a compact symmetric quad-arm meander-line structure that eliminates the need for shorting vias, stacked substrates, or artificial magnetic conductor layers. The antenna employs a geometry-based impedance-tuning mechanism that enables precise conjugate matching with highly capacitive chips such as the UCODE 8/8m chip (15 – j217 Ω at 915 MHz) [23], while maintaining a thin profile of only 0.4 mm and a total footprint of 50 × 50 mm². Moreover, the proposed tag achieves a high power transmission coefficient (≈ 93%) and a read range exceeding 8 m when mounted on metallic surfaces – performance that compares favorably with existing designs while offering lower fabrication cost and simpler integration. These distinctive advantages underscore the novelty and practical value of the present work. Simulations were carried out using Ansoft HFSS software [24], and experimental validation was conducted through fabrication and measurement.

The remainder of this paper is organized as follows: Section 2 presents the configuration of the proposed antenna. Section 3 explains the design methodology and current distribution analysis. Section 4 reports the experimental results.

2. Antenna Structure Configuration

The proposed RFID tag antenna is designed on an FR4 substrate with overall dimensions of L × W = 50 mm × 50 mm and thickness h = 0.4 mm. The dielectric constant of the substrate is $\varepsilon_r = 4.4$, and the loss tangent is approximately 0.02. The antenna is configured to operate in the FCC UHF RFID band (902–928 MHz) for North American applications. The optimized design parameters of the proposed tag antenna are listed in Table 1.

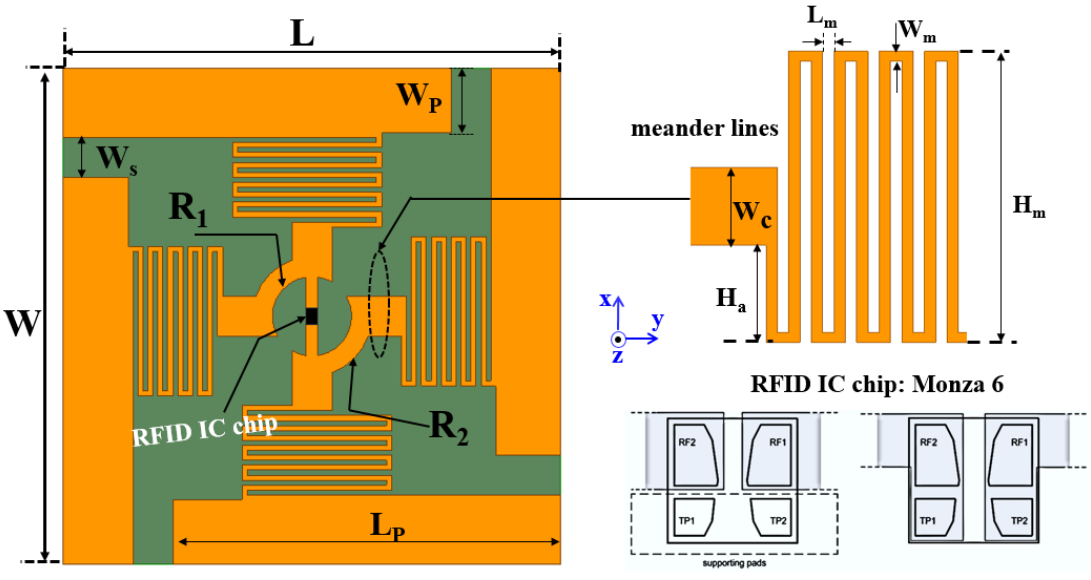

Figure 1. *Structural overview of the proposed antenna on the metallic platform.*

Table 1. *Design parameters of the proposed tag antenna.*

Parameter	Symbol	Value (mm)	Description
Antenna width	W	50	Overall tag width
Antenna length	L	50	Overall tag length
Patch width	W_p	30	Width of each main radiating patch
Patch length	L_p	39	Length of each main radiating patch
Slot width	W_s	4	Coupling slot width for impedance tuning
Radius 1	R_1	4	Corner radius near feed region
Radius 2	R_2	6	Perturbation slot radius
Meander length	L_m	0.5	Length of each meander segment
Meander width	W_m	0.5	Width of each meander line
Meander height	H_m	15	Vertical extent of meander path
Arm height	H_a	5	Height of connecting arm from feed to patch
Dielectric constant	ε_r	4.4	FR4 substrate dielectric constant
Substrate thickness	h	0.4	FR4 thickness

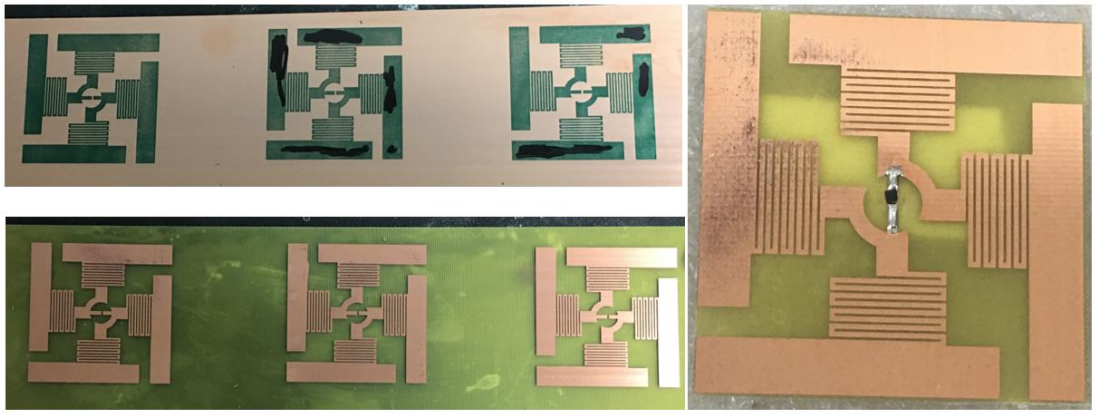

Figure 2. *Layout and fabrication of the proposed antenna incorporating the Ucode 8/8m chip.*

As shown in Figure 1 (antenna geometry) and Figure 2 (fabricated prototype), the radiating structure is symmetrically arranged in a square geometry to achieve good impedance matching and CP radiation. The central feed region accommodates the RFID IC chip (Ucode 8/8m), which is connected through a pair of rectangular supporting pads. These pads ensure reliable soldering and provide a proper electrical interface between the chip terminals (RF1/RF2) and the antenna.

Four radiating arms extend outward from the central feed, each incorporating meander-line sections to increase the effective current path length without enlarging the overall tag size. The meander lines are characterized by length L_m, width W_m, and spacing, which are tuned to control the resonant frequency and input impedance. The connection width W_C links the meander lines to the main radiating patches. Additional tuning parameters include the patch width Wp, patch length Lp, and rectangular slots R_2, which are introduced to perturb the current distribution and generate the necessary directional radiation patterns. The perturbation also improves impedance matching between the antenna and the complex conjugate impedance of the Ucode 8/8m chip.

Overall, the combination of the compact meander lines, perturbation slots, and symmetric geometry ensures that the proposed antenna achieves broad impedance bandwidth, and stable radiation characteristics when mounted on different platforms, including metallic surfaces.

3. Design Procedure And Current Analysis

The design of the proposed compact UHF RFID tag antenna mounted on metallic surfaces follows a systematic approach to ensure proper impedance matching with the Ucode 8/8m chip and stable radiation performance. The main steps of the design methodology are outlined as follows: in the initial configuration, symmetrical meandered slots are introduced on both sides of the central feed region to extend the effective current path and reduce the antenna's resonant frequency without increasing its overall size, as shown in Figure 3a. Figure 3b indicates that the resonant frequency of the antenna is higher than that required; the tag antenna achieves a reactance of j217 Ω at 1220 MHz.

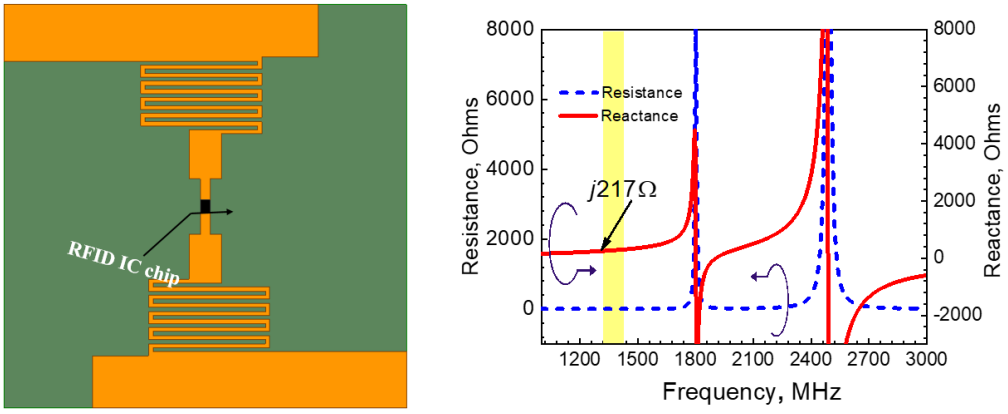

(a) (b)

Figure 3. *(a) the tag structure with symmetrical meandered slots; (b) the input impedance of the antenna configuration.*

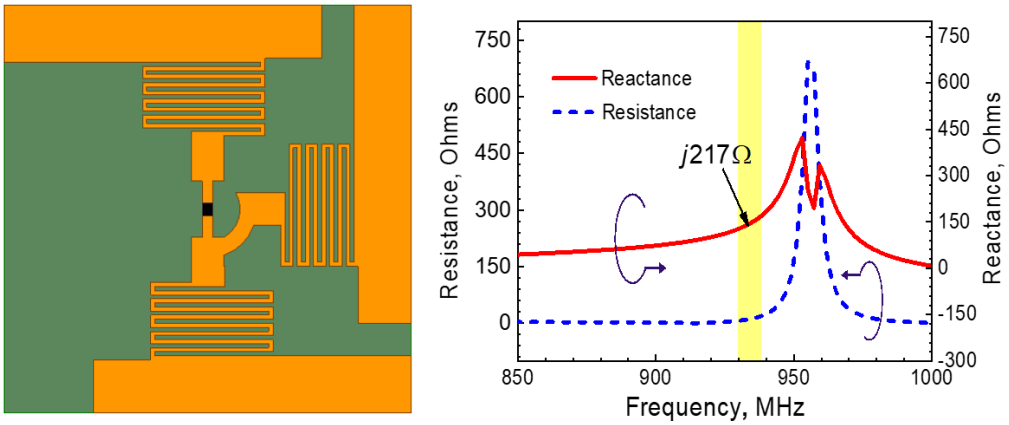

(a) (b)

Figure 4. *(a) the tag structure with the three meandered slots; (b) the input impedance of the antenna configuration.*

To achieve conjugate matching with the UCODE 8/8m IC, which has an input impedance of 13−j217 Ω at 915 MHz, the antenna geometry was modified from the initial structure. As illustrated in Figure 4a, an additional meander-line and curved strip were introduced near the feed region. These modifications increase the effective inductive reactance, thereby compensating for the highly capacitive nature of the IC. Furthermore, the asymmetric meander-line arrangement allows for flexible control of the current distribution and impedance tuning. Therefore, the resonance frequency is reduced from 1220 MHz to 931.5 MHz (see Figure 4b).

To further reduce the antenna size and fine-tune its impedance, four meander-line structures were incorporated symmetrically on both sides of the central feed region, as shown in Figure 5a. The inclusion of these meanders effectively increases the electrical length of the current path without enlarging the

physical footprint of the antenna. This not only supports compactness but also provides additional flexibility in impedance control.

The simulated impedance response is illustrated in Figure 5b. The resistance (dashed line) approaches the target value near 915 MHz, while the reactance (solid line) converges toward j217 Ω, which corresponds to the conjugate of the UCODE 8/8m chip impedance. Compared with previous steps, the introduction of four meander lines enhances the impedance matching condition and ensures more stable resonance around the operating frequency band.

After incorporating four meander-line structures to extend the current path, the antenna impedance was further optimized by adjusting the slot width parameter (W_S), as illustrated in Figure 6a. The variation of W_S directly influences the capacitive coupling between the radiating arms, thereby controlling both the real and imaginary components of the input impedance. The simulated impedance response is shown in Figure 6b. By fine-tuning W_S, the resistance (dashed line) was brought close to the real part of the UCODE 8/8m chip impedance (13 Ω), while the reactance (solid line) converged toward j217 Ω, at 915 MHz. This adjustment yielded an excellent conjugate impedance match between the proposed antenna and the RFID IC chip, ensuring efficient power transfer and stable operation within the FCC band (902–928 MHz).

Thus, the tuning of W_S is a critical step that enables precise impedance matching without significantly increasing antenna size or structural complexity.

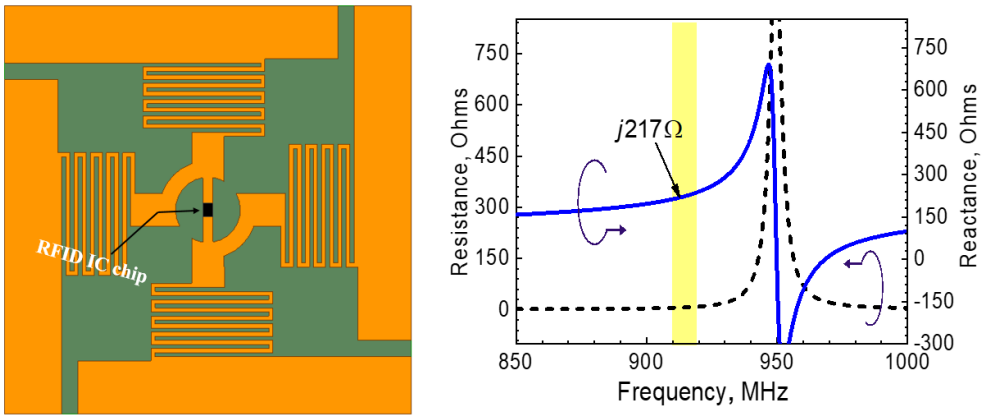

(a) (b)

Figure 5. *(a) the tag structure with the four symmetrical meandered slots; (b) the input impedance of the antenna configuration.*

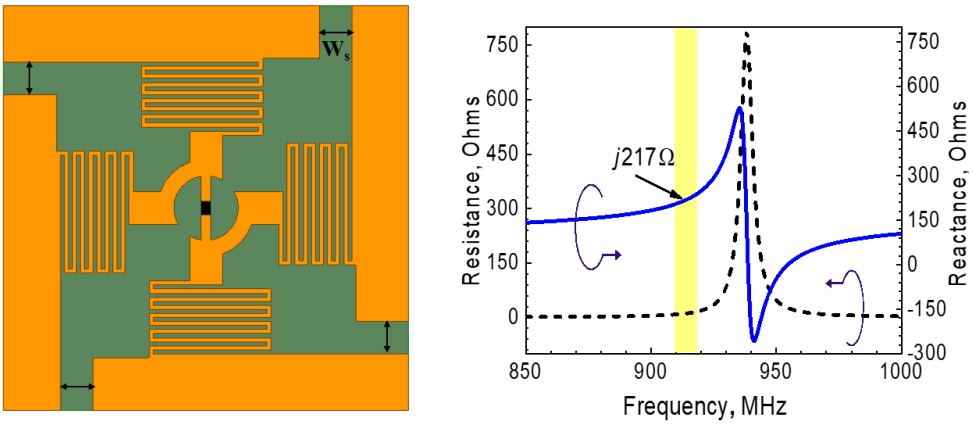

(a) (b)

Figure 6. *(a) geometry of the proposed tag antenna with four symmetrical meandered slots, where the slot width W_s is used to tune the resonant frequency; (b) Simulated input impedance of the antenna, showing resistance (dashed line, left axis) and reactance (solid line, right axis) versus frequency.*

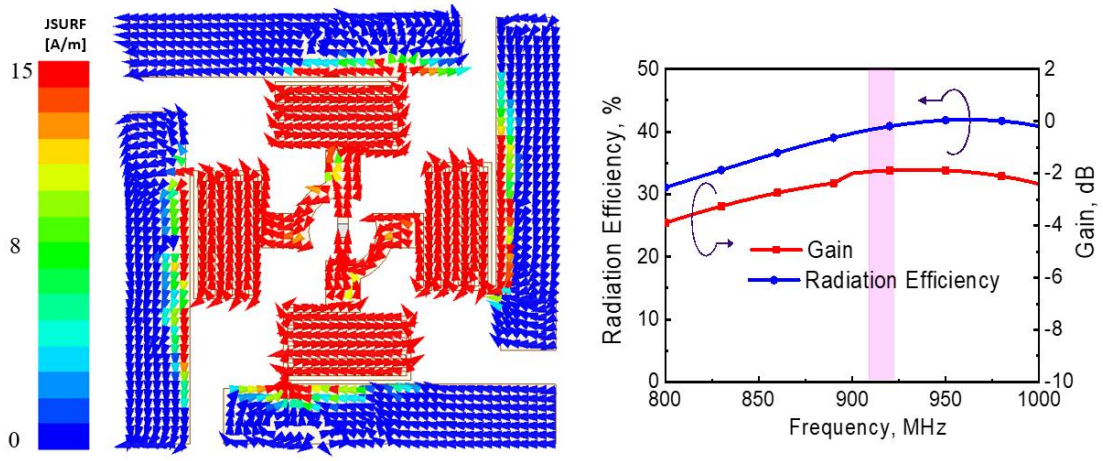

(a) (b)

Figure 7. *The proposed tag antenna with (a) the surface current distribution, (b) radiation efficiency and gain.*

In general, Figure 7 illustrates two key characteristics of the proposed tag antenna. On the left (see Figure 7a), the simulated surface current distribution at 915 MHz is presented when the antenna is mounted on a 250×250 mm^2 metallic plate. The strong current density is clearly concentrated along the four meander-line sections, confirming their dominant role in establishing resonance and fine-tuning the operating frequency.

On the right picture (see Figure 7b), the radiation efficiency and gain are plotted across the 800–1000 MHz frequency range. The antenna exhibits a radiation efficiency exceeding 40% and a peak gain of approximately –1.8 dB within the UHF RFID band (highlighted region around 915 MHz). These results demonstrate that, despite the compact geometry and metal-backed configuration, the proposed design achieves acceptable efficiency and gain performance suitable for practical RFID applications.

4. Experiment And Discussion

The designed UHF RFID tag antenna was realized on an FR4 substrate with a thickness of 0.4 mm, a relative permittivity of 4.4, and a loss tangent of 0.025. The overall antenna dimensions, including the ground plane, were 50 × 50 × 0.4 mm^3. The tag was optimized for integration with a UCODE 8/8m chip, characterized by an input impedance of 15–j217 Ω and a power sensitivity of –22.9 dBm at 915 MHz. To evaluate the antenna performance, the input impedance was measured using a vector network analyzer (VNA) connected to the balun probe via a 50-Ω coaxial cable. The balun was carefully calibrated through open, short, and load standards before conducting the measurements, as described in [25], [26]. Figure 8 compares the simulated and measured input impedance of the antenna when matched to the UCODE 8/8m chip. The measured values were 13+j215 Ω, while the simulated results yielded 11+j219 Ω, both showing a slight deviation from the chip impedance at 915 MHz. To confirm the impedance matching between the antenna and the chip, key performance indicators such as return loss (reflection coefficient) and power transmission coefficient were further analyzed. Following [27], the power wave reflection coefficient (RL) is defined as:

$$RL = \frac{Z_{IC} - Z_{ant}^{*}}{Z_{IC} + Z_{ant}}, 0 \le |RL| \le 1 \quad (1)$$

$$RL(\text{dB}) = -20\log|RL| \quad (2)$$

where

$Z_{IC} = R_{IC} + jX_{IC}$ is the input IC chip impedance.

$Z_{ant} = R_{ant} + jX_{ant}$ is the input antenna structure impedance.

The power delivered to the IC chip is expressed as follows:

$$P_{chip} = \left(1 - |RL|^2\right) P_{ant} \tag{3}$$

where P_{chip} is the power received by the antenna configuration.

To quantify the power transmission coefficient (PTC), the following relation is used:

$$PTC = \frac{P_{chip}}{P_{ant}} = \left(1 - |RL|^2\right) = \frac{4R_{ant}R_{IC}}{\left(R_{ant} + R_{IC}\right)^2 + \left(X_{ant} + X_{IC}\right)^2}, 0 \le RL \le 1 \tag{4}$$

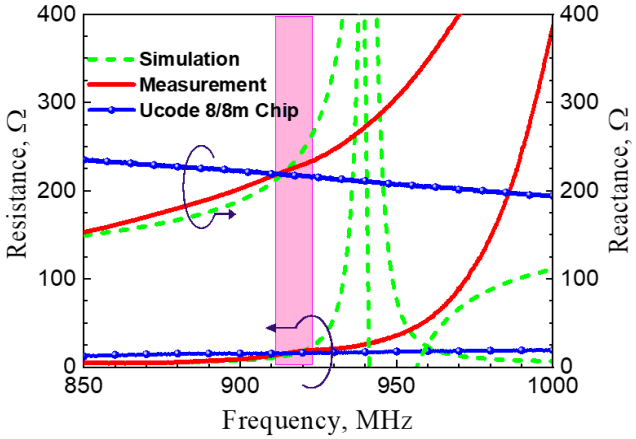

Figure 8. *Input impedance analysis: experimental vs. simulated results for antenna and chip.*

The reflection coefficient and power transmission coefficient (PTC) were determined by substituting the experimentally obtained resistance and reactance values into Equations (1) and (3). Figure 9 presents a comparison of the reflection coefficient and PTC derived from both simulation and measurement. At the resonance frequency, the tag antenna's input impedance closely aligned with that of the chip, indicating effective impedance matching. Nonetheless, the measured 3-dB bandwidth exceeded the simulated one, a variation attributed to fabrication tolerances during the etching process and the influence of cables during measurement—issues also reported in prior research [25], [27]. Additionally, the measured PTC values ranged from 70% to 93% across the FCC-designated operational frequency bands (902–928 MHz) for North America and Vietnam (918.4-923 MHz), further confirming satisfactory impedance matching between the antenna and chip, as shown in Figure 9.

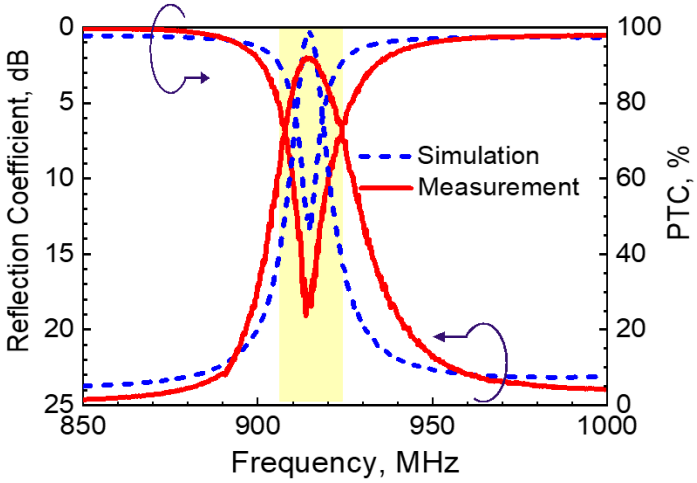

Figure 9. *Comparison between measured and simulated return loss and PTC of the proposed antenna.*

An important metric for assessing the efficiency of the tag antenna is its read range, also referred to as the reading distance. The peak read distance in a radio frequency power link is achieved when the

power received by the chip (P_{chip}) matches the chip's activation threshold (P_{th}), which represents the minimum power required to turn on the RFID tag's microchip [28]:

$$Read\,Range(D) = \frac{\lambda}{4\pi}\sqrt{\frac{P_{reader}G_{reader}G_{ant}\,PTC}{P_{th}}} \quad (5)$$

where

P_{reader} and G_{reader} denote the transmitted power and gain of the reader antenna, respectively. G_{ant} represents the gain of the tag antenna, and while P_{th} refers to the minimum power level required to activate the RFID chip and ensure adequate functionality.

To assess the tag's performance, the equation (5) was employed to estimate the read range. The fabricated tag antenna, mounted on a metallic surface, underwent testing within an anechoic chamber using a measurement setup based on the procedure outlined in [25], [28]. Figures 10a and 10b illustrate the antenna evaluation conducted both inside the chamber and in free space conditions, respectively. The RFID testing configuration comprised a computer, a reader control unit (Favite FS-GM-201), a circularly polarized reader antenna, and the designed tag antenna.

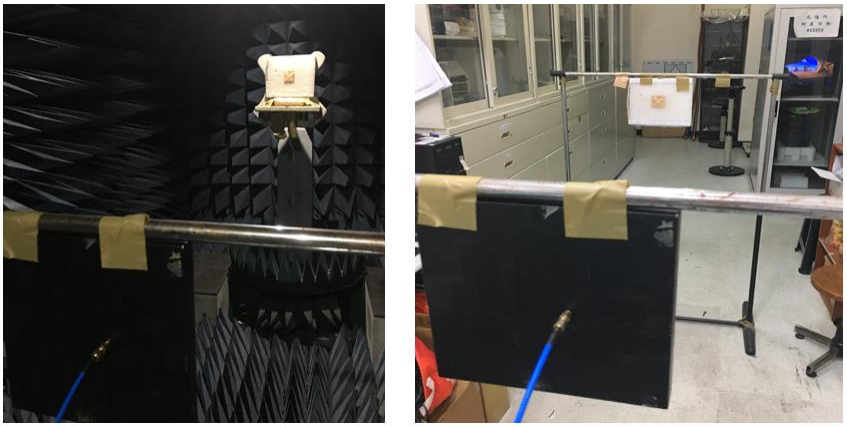

(a) (b)

Figure 10. *Experimental configuration for evaluating RFID tag antenna reading range within (a) the anechoic chamber and (b free space environment.*

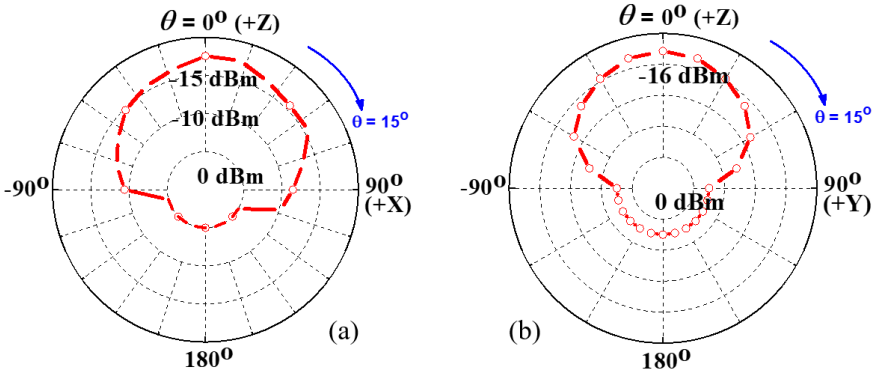

Figure 11. *Angular detection characteristics of the proposed RFID tag antenna at 915 MHz across (a) XZ and (b) YZ planes.*

Figure 11 illustrates the angular sensitivity patterns of the proposed tag antenna at 915 MHz in two orthogonal planes: (a) the XZ plane and (b) the YZ plane. Each polar plot shows how the antenna's sensitivity varies with angle, with signal strength levels marked at 0 dBm, -10 dBm, -15 dBm, and -16 dBm. The red dashed lines represent the measured sensitivity patterns, centered around the maximum response at 0 dBm.

In Figure 11a, the angular distribution is shown in the XZ plane, where 0° corresponds to the +Z direction and 90° aligns with the +X axis. Similarly, Figure 11b presents the pattern in the YZ plane, with 0° along the +Z direction and 90° pointing toward the +Y axis. Both plots include a blue arrow indicating the azimuthal angle φ = 15°, used during measurement. These patterns demonstrate the directional characteristics of the tag antenna and its performance across different orientations.

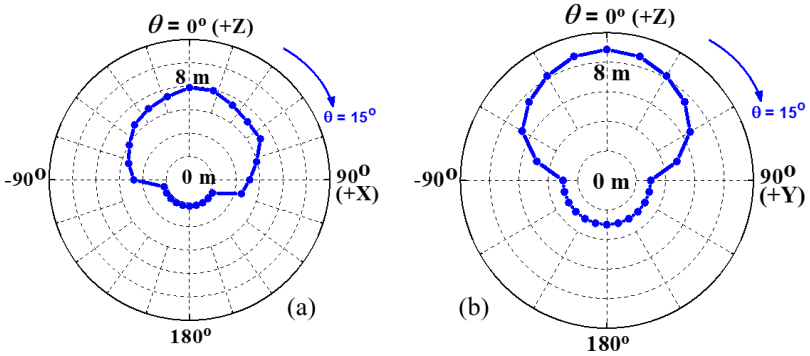

Figure 12. *Experimental reading range results of the proposed RFID tag antenna at 915 MHz in (a) XZ and (b) YZ orientations.*

Figure 12 shows the measured reading range of the proposed tag antenna at 915 MHz in two principal planes: (a) the XZ plane and (b) the YZ plane. Each polar plot illustrates the tag's read distance as a function of angle, with radial markers indicating distances from 0 to 8 meters in 2-meter increments. The blue data points trace the actual reading range achieved during measurement.

In plot Figure 12a, the maximum read distance reaches approximately 7.9 meters in the XZ plane, while Figure 12b shows a peak range of about 8.8 meters in the YZ plane. The angle θ is referenced from 0° in the +Z direction, with 90° corresponding to the +Y and +X directions in plots (a) and (b), respectively. An arrow marks the azimuthal angle θ = 15°, used during the measurement procedure. These results highlight the directional performance of the tag antenna in different spatial orientations.

Table 2 summarizes the performance comparison between the proposed tag antenna and several representative on-metal RFID antennas as well as two commercial products [29], [30]. It can be observed that most existing AMC-based or folded-patch designs achieve reasonable read ranges but require thicker substrates or complex multilayer layouts. In contrast, the proposed symmetric quad-arm meander-line antenna offers a much thinner single-layer structure (0.4 mm) while maintaining a high power-transmission coefficient of about 93 % and a read range exceeding 8 m. These results confirm that the proposed design achieves a balanced combination of compact size, simple fabrication, and competitive performance, making it highly suitable for practical metallic-surface RFID applications.

5. Conclusion and Recommendations

This work presents a compact, symmetric quad-arm meander-line RFID tag antenna specifically designed for metallic surface applications in the UHF band. By integrating a flexible impedance-tuning mechanism and avoiding complex structures such as shorting vias or stacked patches, the proposed antenna achieves efficient conjugate matching with the UCODE 8/8m IC chip. The final design demonstrates a high power transmission coefficient of up to 93% and a maximum read range exceeding 8.0 meters, confirming its suitability for practical RFID deployments.

Experimental results closely match simulation data, validating the effectiveness of the design methodology and confirming stable performance across the FCC frequency band (902–928 MHz) and Vietnam band (918.4–923 MHz). The antenna maintains acceptable radiation efficiency and gain, even when mounted on metal, which is often a challenging environment for RFID tags. Future work may include exploring lower-loss substrate materials to further improve efficiency, extending the design to multi-band or wideband operation for global RFID standards, and integrating the antenna onto flexible or conformal platforms. Additional environmental and mechanical durability tests are also recommended to evaluate long-term performance. Overall, the proposed antenna provides a robust, low-

profile solution for metallic-surface RFID tagging with room for further optimization and broader application.

Table 2. *Comparison of the proposed RFID tag antenna with existing designs and commercial tags*.

Ref./ Design	Antenna Type	Size (mm^3)	Substrate/ Thickness (mm)	Frequency Band (MHz)	Gain (dB)	Efficiency (%)	PTC (%)	Read Range (m)	Key Features/ Limitations
[5]	AMC-based dual-band patch	80 × 80 × 2.0	FR4 / 2.0	865–928	–0.8	55	≈ 85	7.5	Good isolation, but thick and costly AMC substrate
[9]	Slim PIFA	70 × 50 × 1.6	FR4 / 1.6	902–928	–2.5	35	≈ 65	5.0	Thin profile, but narrow bandwidth and poor matching on metal
[18]	Folded patch with inductive stubs	60 × 60 × 1.0	PET / 1.0	915	–1.5	40	≈ 80	6.8	Compact but sensitive to stub placement and adhesive degradation
[20]	Folded patch with orthogonal tuning slots	65 × 65 × 1.6	FR4 / 1.6	902–928	–1.2	45	≈ 85	7.0	Improved tuning, but multi-layer layout increases cost
[22]	Magnetic-loop on-metal tag	55 × 55 × 0.8	FR4 / 0.8	902–928	–2.0	42	≈ 78	7.2	Omnidirectional, but limited impedance-tuning flexibility
[29]	Dipole on-metal	73.3 × 22.8 × 8.3	PET / 0.5	902–928	N/A	N/A	N/A	8	Bulky and expensive
[30]	3-D loop patch	51 x 48 x 12.6	ABS / 3.0	902–928	N/A	N/A	N/A	11	Bulky and expensive
[31]	3-D loop patch	46.5 x 31.5 x 7.5	PPS / 3.3	902–928	N/A	N/A	N/A	6.5	Bulky and expensive
This work	Symmetric quad-arm meander-line	50 × 50 × 0.4	FR4 / 0.4	902–928	–1.8	> 40	≈ 93	8.0 – 8.8	No vias, low-cost single-layer, tunable, high PTC on metal

Acknowledgments

I acknowledge Ho Chi Minh City University of Technology (HCMUT), VNU-HCM for supporting this study.

Conflict of Interest

The author declares no conflict of interest.

REFERENCES

[1] A. Choudhary and D. Sood, "Wideband long range compact serrated triangular patch based UHF RFID tag for metallic base environment," *IEEE Journal of Radio Frequency Identification*, vol. 8, pp. 643–651, 2024.
[2] R. Abdulghafor *et al*., "Recent advances in passive UHF-RFID tag antenna design for improved read range in product packaging applications: A comprehensive review," *IEEE Access*, vol. 9, pp. 63611–63635, 2021.
[3] C. Wu, J. Yuan, and Z. Chen, "A UHF RFID tag antenna placeable on a metal surface without degraded performances," *IEEE Antennas and Wireless Propagation Letters*, vol. 23, pp. 2101–2105, 2024.
[4] R. Xu and Z. Shen, "Wearable ungrounded tag antenna for UHF RFID applications," *IEEE Transactions on Antennas and Propagation*, vol. 71, no. 4, pp. 3665–3670, 2023.
[5] A. Bansal, S. Sharma, and R. Khanna, "Platform tolerant dual-band UHF-RFID tag antenna with enhanced read range using artificial magnetic conductor structures," *Int. J. RF Microw. Comput. Aided Eng.*, vol. 10, pp. 564–574, 2020.
[6] D. Kim and J. Yeo, "Dual-band long-range passive RFID tag antenna using an AMC ground plane," *IEEE Transactions on Antennas and Propagation*, vol. 60, pp. 2620–2626, 2012.
[7] D. Kim and J. Yeo, "Low-profile RFID tag antenna using compact AMC substrate for metallic objects," *IEEE Antennas and Wireless Propagation Letters*, vol. 7, pp. 718–720, 2008.
[8] D. Kim, J. Yeo, and J. I. Choi, "Low-profile platform-tolerant RFID tag with artificial magnetic conductor (AMC)," *Microwave and Optical Technology Letters*, vol. 50, pp. 2292–2294, 2008.
[9] S. L. Chen and K. H. Lin, "A slim RFID tag antenna design for metallic object applications," *IEEE Antennas and Wireless Propagation Letters*, vol. 7, pp. 729–732, 2008.
[10] S. L. Soriano and J. Parron, "Design of a small-size, low-profile, and low-cost normal-mode helical antenna for UHF RFID wristbands," *IEEE Antennas and Wireless Propagation Letters*, vol. 16, pp. 2074–2077, 2017.
[11] G. Marrocco, "The art of UHF RFID antenna design: Impedance-matching and size-reduction techniques," *IEEE Antennas and Propagation Magazine*, vol. 50, pp. 66–79, 2008.
[12] C. H. Loo, K. Elmahgoub, F. Yang, *et al*., "Chip impedance matching for UHF RFID tag antenna design," *Progress in Electromagnetics Research*, vol. 81, pp. 359–370, 2008.
[13] L. Ukkonen and L. Sydänheimo, "Impedance matching considerations for passive UHF RFID tags," in *Proc. Asia Pacific Microwave Conf.*, 2009, pp. 2367–2370.
[14] K. H. Lin, S. L. Chen, and R. Mittra, "A looped-bowtie RFID tag antenna design for metallic objects," *IEEE Transactions on Antennas and Propagation*, vol. 61, pp. 499–505, 2012.
[15] S. L. Chen, "A miniature RFID tag antenna design for metallic objects application," *IEEE Antennas and Wireless Propagation Letters*, vol. 8, pp. 1043–1045, 2009.
[16] C. Y. Chiu, K. M. Shum, and C. H. Chan, "A tunable via-patch loaded PIFA with size reduction," *IEEE Transactions on Antennas and Propagation*, vol. 55, pp. 65–71, 2007.
[17] J. Zhang and Y. Long, "A novel metal-mountable electrically small antenna for RFID tag applications with practical guidelines for the antenna design," *IEEE Transactions on Antennas and Propagation*, vol. 62, pp. 5820–5829, 2014.
[18] W. H. Ng, E. H. Lim, F. L. Bong, and B. K. Chung, "Folded patch antenna with tunable inductive slots and stubs for UHF tag design," *IEEE Transactions on Antennas and Propagation*, vol. 66, pp. 2799–2806, 2018.
[19] B. An, Y. Wu, X. Cai, and F. Wu, "Reliability of RFID tag inlay assembled by anisotropic conductive adhesive," in *Proc. 2nd Electronics System-Integration Technology Conf.*, 2008, pp. 1203–1208.
[20] K. Thirappa, E. H. Lim, F. L. Bong, and B. K. Chung, "Compact folded-patch with orthogonal tuning slots for on-metal tag design," *IEEE Transactions on Antennas and Propagation*, vol. 67, pp. 5833–5842, 2019.
[21] W. H. Ng, E. H. Lim, F. L. Bong, and B. K. Chung, "Compact planar inverted-S antenna with embedded tuning arm for on-metal UHF RFID tag design," *IEEE Transactions on Antennas and Propagation*, vol. 67, pp. 4247–4252, 2019.
[22] S. R. Lee, W. H. Ng, E. H. Lim, F. L. Bong, and B. K. Chung, "Compact magnetic loop antenna for omnidirectional on-metal UHF tag design," *IEEE Transactions on Antennas and Propagation*, vol. 68, pp. 765–772, 2020.
[23] NXP Semiconductors, "SL3S1205/15 datasheet." [Online]. Available: www.nxp.com/docs/en/data-sheet/SL3S1205-15-DS.pdf. Accessed: Sep. 15, 2025.
[24] ANSYS, "ANSYS HFSS." [Online]. Available: www.ansys.com/products/electronics/ansys-hfss. Accessed: Sep. 15, 2025.
[25] M. T. Nguyen, Y. F. Lin, C. H. Chen, C. H. Chang, and H. M. Chen, "Shorted patch antenna with multi slots for a UHF RFID tag attached to a metallic object," *IEEE Access*, vol. 9, pp. 111277–111292, 2021.
[26] M. T. Nguyen, Y. F. Lin, C. H. Chen, H. S. Luong, and H. M. Chen, "Low profile planar inverted-L antenna (PILA) for UHF RFID tag on signal absorption and reflection surfaces," *IEEE Access*, 2025.
[27] M. T. Nguyen, Y. F. Lin, C. H. Chen, Y. C. Tseng, and H. M. Chen, "Miniature 3-D dipole antenna for UHF RFID tag mounted on conductive materials," *IEEE Transactions on Antennas and Propagation*, vol. 70, no. 12, pp. 11454–11464, 2022.
[28] N. C. Zhi, *Antenna for Portable Devices*. Hoboken, NJ: John Wiley & Sons, 2007.
[29] RF MobiStore, "Xerafy RTI Trak RFID Tag." [Online]. Available: https://rfmobistore.com/collections/metal-mount-rfid-tags/products/xerafy-rti-trak-rfid-tag. Accessed: Nov. 12, 2025.
[30] RFID Solution, "Omni-ID Exo 750 RFID Tag." [Online]. Available: https://rfidsolution.com.vn/omni-id-exo-750-rfid-tag-pack-of-10. Accessed: Nov. 12, 2025.
[31] RF MobiStore, "RFMobi concrete-embedded RFID tag TMOP4601." [Online]. Available: https://rfmobistore.com/collections/metal-mount-rfid-tags/products/rfmobi-concrete-embedded-rfid-tag-tmop4601. Accessed: Nov. 12, 2025.

Minh Tan Nguyen received a B.S. degree in Electronic Physics and an M.S. degree in Electronics and Telecommunication Engineering from Vietnam National University Ho Chi Minh City in 2007 and 2013, respectively, and the Ph.D. degree in Electronic Engineering from National Kaohsiung University of Science and Technology (NKUST), Taiwan in 2023. Under the guidance of his Advisor, he has been awarded the Best Student Paper Award in the 2020 IEEE International Workshop on Electromagnetics: Applications and Student Innovation Competition (IEEE IWEM 2020). Since 2023, he has been a Visiting Researcher at the Institute of Photonic Engineering, NKUST, Taiwan. He is also a Lecturer in the Department of Telecommunication, Faculty of Electrical and Electronics Engineering, Ho Chi Minh University of Technology, VNU-HCM. His main research interests include antenna design for RFID Tags, Reader, Phase Array Antennas, 5G/ 6G base stations.
Email: nmtan@hcmut.edu.vn. ORCID: https://orcid.org/0000-0002-2274-4292